Defence Research and Development Canada
Recherche et développement pour la défense Canada

DEFENCE R&D DÉFENSE

# Low cost guidance and control solution for in-service unguided 155 mm artillery shell

*Eric Gagnon*
*Marc Lauzon*
*DRDC Valcartier*

**Defence R&D Canada – Valcartier**
Technical Report
DRDC Valcartier TR 2008-333
July 2009

Canada

# Low cost guidance and control solution for in-service unguided 155 mm artillery shell

Eric Gagnon
Marc Lauzon
DRDC Valcartier

**Defence R&D Canada – Valcartier**

Technical Report
DRDC Valcartier TR 2008-333
July 2009

Principal Author

*Original signed by Eric Gagnon*

Eric Gagnon

Scientist

Approved by

*Original signed by Alexandre Jouan*

Alexandre Jouan

Head, Precision Weapons Section

Approved for release by

*Original signed by Christian Carrier*

Christian Carrier

Chief Scientist

# Abstract

Guidance and control of artillery projectiles will be critical to future military operations. With the large quantities of unguided artillery shells stockpiled around the world, the course correction fuze could provide an attractive and cost-effective solution for munition control. This report proposes a drag brake and a spin brake course correction fuze concept, and compares their performance against the roll-decoupled four canard configuration. Specific guidance and control functions were designed and tuned for each using the 155 mm spin-stabilized artillery projectile as baseline. Dispersion sources included variations in muzzle velocity and gun's azimuth and elevation angles relative to nominal conditions, and wind velocity perturbations. Monte Carlo simulations were performed to analyze the delivery accuracy. Results show that the drag brake concept compensates for muzzle velocity and longitudinal wind perturbations efficiently. The spin brake concept compensates for perturbations in lateral wind efficiently and, to a lesser extent, in the gun's azimuth. The roll-decoupled four canard configuration counteracts gun's azimuth and elevation perturbations very well. A course correction fuze combining the drag brake and spin brake concepts is shown to be a good solution to increase the projectile accuracy when all disturbances studied are present.



# Résumé

Le guidage et le contrôle des projectiles d'artillerie sera important pour les opérations militaires futures. Avec la grande quantité de projectiles d'artillerie non guidés entreposés à travers le monde, les fusées à correction de trajectoire pourraient fournir une solution attrayante et peu coûteuse pour contrôler des munitions. Ce rapport propose un concept de fusée à correction de trajectoire avec frein aérodynamique et un autre concept de fusée avec frein de roulis, et compare leurs performances avec la configuration découplée en roulis et possédant quatre canards. Des fonctions de guidage et de contrôle spécifiques ont été conçues et ajustées pour chaque concept, utilisant le projectile d'artillerie typique stabilisé par roulis de 155 mm comme concept de base. Les sources de dispersion sont des variations sur la vitesse à la bouche et sur l'azimut et l'élévation du canon par rapport aux conditions nominales, et des perturbations sur la vitesse du vent. Des simulations Monte Carlo ont été effectuées pour analyser la précision du projectile à la cible. Les résultats montrent que le concept avec frein aérodynamique compense efficacement les perturbations sur la vitesse à la bouche et sur le vent longitudinal. Le concept avec frein de roulis compense efficacement les perturbations sur le vent latéral, et en moindre importance, les perturbations sur l'azimut du canon. La configuration découplée en roulis et possédant quatre canards agit très bien contre les perturbations sur l'azimut et l'élévation du canon. Une fusée à correction de trajectoire combinant les concepts avec frein aérodynamique et frein de roulis apparaît comme une bonne solution pour augmenter la précision du projectile lorsque toutes les perturbations étudiées sont présentes.

This page intentionally left blank.

# Executive summary

## Low cost guidance and control solution for in-service unguided 155 mm artillery shell

**Eric Gagnon; Marc Lauzon; DRDC Valcartier TR 2008-333; Defence R&D Canada – Valcartier; July 2009.**

Guidance and control of artillery projectiles will be an important asset in future military operations. As a result, different projects are under way in several countries with the objective to develop and field precision guided artillery munitions. With the large quantities of unguided artillery shells stockpiled around the world, course correction fuzes could provide an attractive and cost-effective solution to achieve munition guidance. This report proposes drag brake and spin brake course correction fuze concepts, separate and combined, and compares their performance with the concept of a roll-decoupled course correction fuze controlling four canards.

This work was accomplished with the objective of building a knowledge base on advanced artillery projectiles in Canada, and for studying course correction fuze concepts to achieve clear improvements in accuracy of in-service conventional projectiles which are stockpiled in large quantities around the world. This work was conducted under Project 12qj "Concept development of artillery precision guided munitions", and represents the continuation of the course correction fuze work started under Project 12qe17 "Integrated Advanced Munition Concept". Project 12qe17 aimed at studying how advanced technology integration could improve effectiveness, in the areas of explosives, guidance and control, and the addition of a propulsion system. The current project 12qj seeks to develop and integrate precision guided weapon technologies from DRDC and Canadian defence industry.

The concept development and evaluation were performed using a 6DOF model of a typical 155 mm spin-stabilized artillery projectile. The 155 mm shell is currently a munition of choice in military organizations due to its interesting range and effect on target. Furthermore, the standard NATO two-inch thread of a 155 mm projectile is large enough to consider the packaging of a course correction fuze with technologies available today. Specific guidance and control functions were designed and tuned for the concepts studied. Linear and nonlinear six-degree-of-freedom models of the projectile were used to develop and tune the guidance and control functions, and to simulate the guided and non-guided projectile. The concepts were analyzed as a function of muzzle velocity, lateral and longitudinal wind velocity, and gun's azimuth and elevation perturbations. Monte Carlo simulations were performed to analyze the precision on target provided by each course correction fuze concept. Results show that the drag brake concept compensates for muzzle velocity and longitudinal wind velocity perturbations efficiently. The spin brake concept compensates for lateral wind velocity perturbations efficiently and reduces significantly the gun's azimuth perturbation effect. The roll-decoupled course correction fuze with four canards is very efficient to counteract the gun's azimuth and elevation perturbations. However, a course correction fuze combining the drag brake and spin brake concepts appears as the best choice to decrease the lateral and longitudinal dispersion when all disturbances studied are present.

# Sommaire

## Low cost guidance and control solution for in-service unguided 155 mm artillery shell

**Eric Gagnon; Marc Lauzon; DRDC Valcartier TR 2008-333; R & D pour la défense Canada – Valcartier; Juillet 2009.**

Le guidage et le contrôle des projectiles d'artillerie représentera un avantage important pour les opérations militaires futures. Par conséquent, plusieurs projets sont en chantier dans différents pays avec l'objectif de développer et réunir des munitions d'artillerie guidées de précision. Avec la grande quantité de projectiles d'artillerie non guidés entreposés à travers le monde, les fusées à correction de trajectoire pourraient fournir une solution attrayante et peu coûteuse pour obtenir des munitions guidées. Ce rapport propose des concepts de fusées à correction de trajectoire avec frein aérodynamique et frein de roulis, et compare leurs performances avec le concept d'une fusée à correction de trajectoire découplée en roulis et contrôlant quatre canards.

Ce travail a été accompli avec l'objectif de constituer une base de connaissances sur les projectiles d'artillerie avancés au Canada, et de trouver un concept de fusée à correction de trajectoire qui pourrait réellement améliorer la précision des projectiles conventionnels en service qui sont entreposés en grande quantité à travers le monde. Ce travail a été réalisé dans le cadre du projet 12qj intitulé "Développement de concepts de munitions guidées de précision pour l'artillerie", et représente la suite du travail sur les fusées à correction de trajectoire entrepris dans le projet 12qe17 intitulé "Concept de munition avancée intégrée". Le projet 12qe17 étudiait comment l'intégration de technologies avancées pourrait améliorer l'efficacité, dans les secteurs de la propulsion, des matériaux énergétiques, du guidage et du contrôle. Le projet 12qj vise à développer et intégrer les technologies des armes guidées de précision de RDDC et de l'industrie de la haute technologie canadienne.

L'analyse a été réalisée avec un projectile d'artillerie typique stabilisé par roulis de 155 mm. La munition de 155 mm a une portée intéressante et produit un effet significatif à la cible. De plus, le filet standard de deux pouces de l'OTAN pour un projectile de 155 mm est assez grand pour considérer l'emballage d'une fusée à correction de trajectoire avec les technologies disponibles aujourd'hui. Des fonctions de guidage et de contrôle spécifiques ont été conçues et ajustées pour les concepts étudiés. Des modèles linéaire et non linéaire à six degrés de liberté du projectile ont été utilisés pour développer et ajuster les contrôleurs des fonctions de guidage et de contrôle, et pour simuler le projectile guidé et non guidé. Les concepts ont été analysés en fonction de perturbations sur la vitesse à la bouche du canon, la vitesse latérale et longitudinale du vent, et l'azimut et l'élévation du canon. Des simulations Monte Carlo ont été effectuées pour analyser la précision à la cible produite par chaque concept de fusée à correction de trajectoire. Les résultats montrent que le concept avec frein aérodynamique compense les perturbations sur la vitesse à la bouche du canon et la vitesse longitudinale du vent de façon efficace. Le concept avec frein de roulis compense les perturbations sur la vitesse latérale du vent de façon efficace et réduit l'effet des perturbations sur l'azimut du canon de façon significative. La fusée à correction de trajectoire découplée en roulis avec quatre canards est très efficace pour contrer les actions des perturbations sur l'azimut et l'élévation du canon. Cependant, une fusée à correction de trajectoire combinant les concepts de frein aérodynamique et frein de roulis apparaît comme le meilleur choix pour

réduire la dispersion latérale et longitudinale lorsque toutes les sources de perturbations étudiées sont présentes.

This page intentionally left blank.

# Table of contents

# List of figures

# List of tables

This page intentionally left blank.

# 1 Introduction

An important objective for future artillery projectiles is a higher delivery accuracy, leading to improved effects with reduced round expenditure. Interesting concepts under study at the moment in several countries aim to retrofit existing stockpiles with course correction fuzes (CCF). Some CCF concepts consider drag brakes to obtain rough range corrections. This includes the French program SPACIDO [1] (Système à Précision Améliorée par CInémomètre DOppler) that aims at developing a fuze deploying triple D-ring plates. The German TCF (Trajectory Correction Fuze) concept [2] uses an umbrella-shaped drag brake. The United Kingdom program STAR [3] (Smart Trajectory Artillery Round) deploys a number of drag plates, and the United States LCCM (Low-Cost Competent Munitions) program [4] uses four D-rings mounted on sliding rails [5], [6]. These fuzes, shown in Fig. 1, fit into the standard NATO two-inch thread of a 155 mm projectile. Other CCF concepts offer both range and lateral corrections. In this area, two projects from the United States aim, respectively, at developing a fuze deploying two grid fins [7] in one case, and two drag brakes and a spin brake [8] in the other case. The United States worked also on a CCF concept with four canards [9]. These more advanced concepts are shown in Fig. 2.

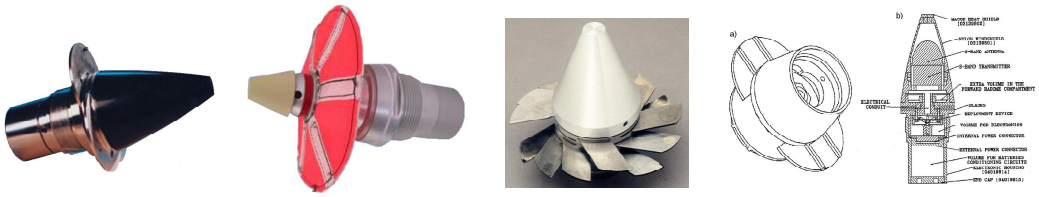

SPACIDO (French) TCF (German) STAR (UK) LCCM (US)

*Figure 1: CCF concepts to obtain range corrections*

Four canards concept (US)

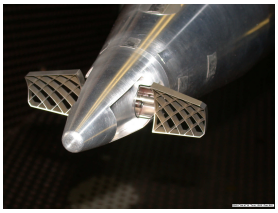

Two grid fins concept (US)


Drag brakes and spin brake concept (US)

*Figure 2: CCF concepts to obtain both range and lateral corrections*

DRDC conducted three analytical studies on CCF. The first study reviewed and confirmed the existence of technological options and those in development to achieve accuracy [10]. The second study looked at possible one-dimensional (1D) corrections when using the drag brake, and achievable two-dimensional (2D) corrections when using impulse jets [11]. The concept of a roll-decoupled CCF, providing corrections in both azimuth and elevation planes using four canards, was analyzed in a third study [12], [13].

The present report proposes drag brake and a spin brake CCF concepts and compares their performance against the one initially proposed by Regan and Smith [9] of a roll-decoupled CCF with four canards. Some papers [14], [15], [16] have shown that canards could be an appropriate control solution to correct both longitudinal and lateral probable errors (PE). Drag and spin brake CCF concepts on the other hand can each reduce only one of the two error component, namely the longitudinal or the lateral one, respectively. The two CCF concepts studies here use braking systems with continuous feedback control, which provides a more effective control than with those systems which cannot be retracted or their positions modulated. The two concepts were evaluated separately but also combined, resulting in either one and two-degree-of-freedom (2DOF) guidance. All CCF concepts were evaluated for their effectiveness to reduce dispersion at impact due to perturbations in muzzle velocity, gun's azimuth and elevation, and longitudinal and lateral wind velocity. Monte Carlo simulations were performed to assess the delivery accuracy.

A typical 155 mm spin-stabilized artillery projectile was used to perform the present analysis. A generic full nonlinear six-degree-of-freedom (6DOF) simulation model was configured accordingly. A linear version of this model was also produced to support the required design and tuning of the guidance and control functions. The guidance and control functions were designed using linear control theory, and tuned with standard loop-shaping techniques. Gain scheduling was used to take into account the projectile's airspeed variation over its trajectory for the roll-decoupled CCF with four canards.

The guidance and control strategies found in the literature to improve artillery projectile accuracy can be divided into three categories. The first category includes methods which carry out predictions of the impact point during flight and make corrections accordingly [14], [17], [18], [19]. These methods can be used to determine the deployment time of the braking systems, the activation time of the pulse jets or the deflection of the control surfaces. It should be noted that an accurate prediction of the impact point in real time for high tempo feedback control requires a fair computing power, which is deemed incompatible with low-cost volume-constrained course correction munitions. The second category includes those methods which perform trajectory shaping [14], [20], [21], [22], but one drawback is the high energy expenditure in following non-ballistic trajectories. The result is an energy-inefficient actuation force distribution over the trajectory, which can produce undesired actuator saturations. The third category contains those methods which carry out trajectory tracking [12], [13], [15], [16], [22], [23]. These methods assume that the tracked trajectory is uploaded into the projectile prior to or at launch, and followed in flight to achieve accuracy. Ballistic trajectory tracking involves less guidance corrections than other trajectory tracking, which contributes to maintaining a low drag, hence a higher average airspeed, and to reduce the occurrence of actuator saturation conditions. This method requires low computing power and makes use of the standard firing tables providing impact data for a given shell under different muzzle velocity, angle of launch and environmental conditions. The guidance and control strategies proposed in this report are based on ballistic trajectory tracking, so they fall into the third category.

The results of the analysis indicated that a combination of the proposed drag and spin brakes was the more promising configuration. The drag brake compensates for muzzle velocity and longitudinal wind perturbations. The spin brake compensates for lateral wind perturbations efficiently and reduces significantly the effect of launch azimuth perturbations. The roll-decoupled CCF with four canards compensates for the gun's azimuth and elevation perturbations. However, the proposed CCF combining the drag and spin brake concepts is the better choice overall, when all studied perturbations are present.

In this document, Chapter 2 presents the reference coordinate systems used. Chapter 3 describes the projectile studied. Chapter 4 explains the concept of a roll-decoupled CCF with four canards. Chapter 5 and Chapter 6 present, respectively, the drag brake and spin brake concepts proposed. The simulation results and analysis are shown in Chapter 7, and conclusions and recommendations are provided in Chapter 8.

# 2 Reference coordinate systems

The development of the guided spin-stabilized projectile concepts requires a careful selection of the reference coordinate systems for stability and guidance and control analysis/synthesis and also for onboard computation and mechanization [24]. Three reference coordinate systems were used in the present analysis:

- Flat earth frame
- Body frame
- Body frame non-spinning

The flat earth frame is a standard approximation of the earth inertial reference frame, and is sufficiently accurate for flights over short ranges. It is a fixed, non-rotating reference frame, and neglects the earth's curvature and rotation that otherwise produces Coriolis and rotational forces on the air vehicle. Its $x$ and $y$ axes are in the horizontal plane and its $z$-axis is normal to the $x$-$y$ plane and pointing down. The origin of the flat earth reference frame was set at the end of the gun tube, as shown in Fig. 3, since it was the starting point of the 6DOF simulations.


*Figure 3: Flat earth reference coordinate system*

The body frame is fixed to the projectile with its origin at the projectile center of mass. When its Euler roll angle is zero, as shown in Fig. 4, its positive $x$-axis aligns with the projectile centerline and points forward out of the nose, its positive $y$-axis points to the right, and its $z$-axis, down. Figure 4 also defines the two components of the total angle of attack ($\alpha$,$\beta$), the velocity vector of the projectile ($u$,$v$,$w$) and its angular velocity vector ($p$,$q$,$r$). The body frame non-spinning is similar to the body frame, but does not spin with the airframe. Its Euler roll angle remains zero at all times.

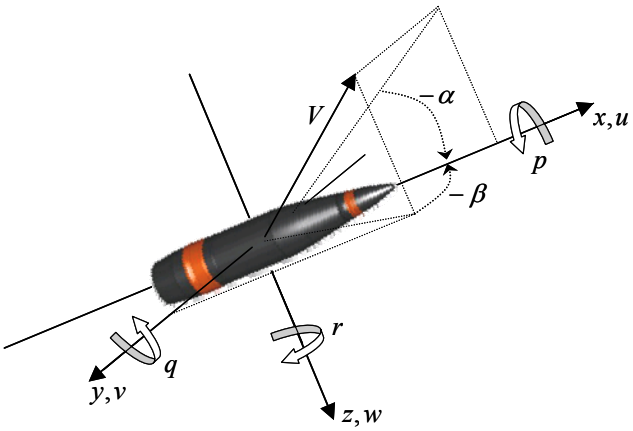


*Figure 4: Body frame coordinate system*

# 3 Projectile studied

The CCF concept development and analysis were conducted using a typical 155 mm spin-stabilized artillery projectile. Compared with smaller caliber projectiles, the 155 mm provides a reasonable fuze volume to package current CCF designs with today's technologies. The full nonlinear 6DOF model was used to simulate the behaviour of the projectile with the application of guidance and control forces and moments. A linear version of the nonlinear 6DOF model was formulated to support the design and tuning of guidance and control functions required in the CCF concepts under study.

## 3.1 Linear 6DOF model

This section describes the linear 6DOF model used, which is based on the well-known nonlinear equations of motion [25], [26]. The nonlinear equations of motion are readily solved with a digital computer using an appropriate numerical integration scheme. Using a set of assumptions, the nonlinear equations can be further simplified to a set of linear equations. When the assumptions are satisfied, the linear equations can then be used to obtain analytical solutions of sufficient accuracy for guidance and control designs. The linear model of this report was obtained using the following assumptions:

- Small angles of attack and sideslip
- Constant speed and roll rate
- Symmetrical projectile, so nil products of inertia and equal non-axial moments of inertia ($I_z = I_y$)
- Gravity omitted

Based on the previous assumptions, the following approximations can be defined:

$$\begin{aligned} u &\approx V \\ \alpha &\approx w/u \approx w/V \\ \beta &\approx -v/u \approx -v/V \end{aligned} \tag{1}$$

$$\begin{aligned} \dot{\alpha} &\approx \dot{w}/u \approx \dot{w}/V \\ \dot{\beta} &\approx -\dot{v}/u \approx -\dot{v}/V \end{aligned} \tag{2}$$

and the linear equations of motion in the body frame can be written as:

$$\begin{aligned} \dot{p} &= F_s d/2I_x \\ \dot{q} &= M_q q + M_\alpha \alpha - pM_{P\alpha}\beta - x_{cg}F_z/I_y + M_{\dot{\alpha}}\dot{\alpha} + pr\left(I_y - I_x\right)/I_y \\ \dot{r} &= M_q r + M_\alpha \beta + pM_{P\alpha}\alpha + x_{cg}F_y/I_y + M_{\dot{\alpha}}\dot{\beta} - pq\left(I_y - I_x\right)/I_y \end{aligned} \tag{3}$$

$$\begin{aligned}\dot{u} &= F_x/m \\ \dot{v} &= -Z_\alpha V\beta + F_y/m - Vr + pw \\ \dot{w} &= Z_\alpha V\alpha + F_z/m + Vq - pv\end{aligned} \tag{4}$$

where the rate of change of the body frame angles of attack and sideslip can be written as:

$$\begin{aligned}\dot{\alpha} &= Z_\alpha \alpha + F_z/mV + p\beta + q \\ \dot{\beta} &= Z_\alpha \beta - F_y/mV + r - p\alpha\end{aligned} \tag{5}$$

and where the dimensional aerodynamic coefficients are defined as:

$$\begin{aligned}Z_\alpha &= -QSC_{L\alpha}/mV \\ M_\alpha &= QSdC_{m\alpha}/I_y \\ M_q &= QSd^2C_{mq}/2VI_y \\ M_{P\alpha} &= QSd^2C_{mP\alpha}/2VI_y \\ M_{\dot{\alpha}} &= QSd^2C_{m\dot{\alpha}}/2VI_y\end{aligned} \tag{6}$$

The external control forces $F_s$, $F_x$, $F_y$ and $F_z$ are applied at the nose of the projectile. $F_y$ and $F_z$ induce moments about the center of gravity, with a moment arm denoted as $x_{cg}$. $F_s$ induces a roll moment to control the roll rate, with an arbitrarily moment arm corresponding to the shell reference diameter $d$.

## 3.2 Physical properties

The full nonlinear 6DOF model of this report uses the nominal physical properties of a typical 155 mm spin-stabilized projectile [27]. These properties are listed in Table 1. In practice, shell physical properties can vary slightly from round to round, but CCF robustness is outside the scope of the present analysis.

*Table 1: Projectile physical properties*

| Parameter | Value |
|---|---|
| $d$ | 0.15474 m |
| $S$ | 0.01881 $m^2$ |
| $x_{cg}$ | 0.55 m |
| $l$ | 0.8735 m |

| | |
|---|---|
| $m$ | 42.989 Kg |
| $I_x$ | 0.1472 Kg m$^2$ |
| $I_y$ | 1.89277 Kg m$^2$ |
| $p$ | 1668 rad/s |

## 3.3 Aerodynamic coefficients

The non-dimensional coefficients $C_{L\alpha}$, $C_{m\alpha}$, $C_{mq}$ and $C_{m\dot{\alpha}}$ in Table 2 were obtained using the aero-prediction software Missile DATCOM 02, based on the dimensions of the nominal 155 mm projectile without actuator (Table 1). The presence of actuators was considered only in the external force and moment terms in the 6DOF equations of motion. Note that the coefficients $C_{L\alpha}$ and $C_{m\alpha}$ were linearized at the trim point $\alpha$=0, and the coefficient $C_{mP\alpha}$ was neglected.

*Table 2: Non-dimensional aerodynamic coefficients*

| Mach | $C_{L\alpha}$ | $C_{m\alpha}$ | $C_{mq}$ | $C_{m\dot{\alpha}}$ |
|---|---|---|---|---|
| 2.5 | 2.655 | 3.667 | -12.273 | -0.122 |
| 2 | 2.464 | 3.953 | -12.178 | -0.123 |
| 1.5 | 2.063 | 4.163 | -11.394 | -0.119 |
| 1.1 | 1.872 | 4.183 | -10.245 | -0.162 |
| 0.95 | 1.642 | 5.195 | -7.928 | -0.125 |
| 0.9 | 1.547 | 4.775 | -7.296 | -0.115 |
| 0.6 | 1.413 | 4.202 | -4.634 | -0.073 |

# 4 Roll-decoupled CCF with canards

This CCF concept initially proposed by Regan and Smith [9] provides course correction in both azimuth and elevation planes. In this concept, it is assumed that the fuze contains the required sensors to provide accurate position and attitude information. The fuze is also equipped with four small control surfaces (canards) for controllability. The CCF is decoupled and counter rolled from the projectile body, so that guidance and control is carried out with continuously applied commands that do not spin with the airframe and therefore do not need to be modulated at the spin frequency. The guidance and control algorithms therefore use non-rolling inertial measurements of the airframe. A coupled fuze-body would impose extreme specifications on sensors and actuators given the high spin rate of the projectile. The fuze finally contains a microprocessor on which the guidance and control algorithms are implemented.

In the present analysis, the actuators were not modeled in detail; rather, external forces were specified and applied on the guided projectile nose. The aerodynamics of the guided and unguided projectiles were considered identical. The external control forces were applied along the *y* and *z* axes of the body frame non-spinning coordinate system.

## 4.1 Projectile control

The purpose of the control function is to ensure flight stability despite the application of control forces on the projectile nose. In fact, the application of these forces generates nutation and precession behaviors. Lloyd and Brown [28] have shown that a typical 105 mm shell can become dynamically unstable with a steady horizontal or vertical control force applied on the nose.

Linear control theory based on decentralized controllers tuned with standard loop-shaping techniques was used to develop the projectile control function. The pitch and yaw rates in the body frame non-spinning coordinate system were selected as the output variables, specifically to dampen the undesirable nutation and precession behaviors.

In order to apply the linear control theory to design the control function, the linearization of the nonlinear transformations between the body frame and body frame non-spinning is required. This linearization can not be solved analytically, so an identification of the projectile linear model in the body frame non-spinning was performed. The output error method [29] and Eqs. (3), (4) and (5) were used to conduct this identification. The output error method compares the nonlinear model output data with that of the linear model using the same excitation signal. The parameters of the linear model are tuned to minimize the error between the model outputs. The best results were obtained with the transfer functions shown in Eqs. (7) and (8). The transfer function parameters for different Mach numbers at sea level are listed in Table 3.

$$\frac{q^*(s)}{F_y^*(s)} = \frac{r^*(s)}{F_z^*(s)} = \frac{K_1 s^2}{\left(s^2 + 2\zeta_1\omega_1 s + \omega_1^2\right)\left(s^2 + 2\zeta_2\omega_2 s + \omega_2^2\right)} \tag{7}$$

$$\frac{r^*(s)}{F_y^*(s)} = -\frac{q^*(s)}{F_z^*(s)} = \frac{K_2\left(s^2 + 2\zeta_3\omega_3 s + \omega_3^2\right)\left(\frac{-s}{\omega_1}+1\right)\left(\frac{s}{\omega_2}+1\right)}{\left(s^2 + 2\zeta_1\omega_1 s + \omega_1^2\right)\left(s^2 + 2\zeta_2\omega_2 s + \omega_2^2\right)\left(\frac{s}{\omega_1}+1\right)} \tag{8}$$

*Table 3: Parameters of the projectile linear model in the body frame non-spinning coordinate system*

| Mach | $K_1$ | $K_2$ | $\omega_1$ | $\zeta_1$ | $\omega_2$ | $\zeta_2$ | $\omega_3$ | $\zeta_3$ |
|---|---|---|---|---|---|---|---|---|
| 2.5 | -38 | -30 | 23.55 | 0.03 | 106.2 | 0.0064 | 2.99 | 1 |
| 2 | -38 | -30 | 15.05 | 0.035 | 114.7 | 0.0047 | 2.03 | 1 |
| 1.5 | -38 | -30 | 8.43 | 0.04 | 121.3 | 0.0031 | 1.1 | 1 |
| 1.1 | -38 | -30 | 4.405 | 0.055 | 125.314 | 0.0018 | 0.61 | 1 |
| 0.95 | -38 | -30 | 4.07 | 0.045 | 125.65 | 0.0012 | 0.28 | 1 |
| 0.9 | -38 | -30 | 3.33 | 0.041 | 126.4 | 0.00105 | 0.26 | 1 |
| 0.6 | -38 | -30 | 1.28 | 0.075 | 128.45 | 0.00043 | 0.14 | 1 |

Once the linear model in the body frame non-spinning is identified, it is possible to choose the airframe input-output pairing for the control loops. It is important to pick the best choice over all Mach numbers flown by the projectile. The projectile linear model in the body frame non-spinning was simulated to compare the temporal results for control forces on $F_y^*$ and $F_z^*$ at the Mach numbers studied. These temporal results showed that $F_z^*$ has a higher effect on $q^*$ and $F_y^*$ on $r^*$ for all Mach numbers studied.

Decentralized controllers were designed for the pairing chosen using standard loop-shaping techniques [30], [31]. The pairing $q^*$ with $F_z^*$ and $r^*$ with $F_y^*$ being the most appropriate, controllers were designed for the transfer functions presented in Eq. (8) without taking into account the interaction produced by the cross transfer functions of Eq. (7). The resulting controllers are:

$$C_{r*}(s) = -C_{q*}(s) = \frac{K_3\left(s^2 + 2\zeta_1\omega_1 s + \omega_1^2\right)\left(s^2 + 2\zeta_2\omega_2 s + \omega_2^2\right)}{s\left(s^2 + 2\zeta_3\omega_3 s + \omega_3^2\right)\left(\frac{s}{\omega_2}+1\right)} \tag{9}$$

These controllers were designed to cancel the complex poles, the complex zeros and a real zero in Eq. (8). For each controller, an integrator was added and the gain $K_3$ tuned initially to obtain a desired phase margin of 60°. Each controller gain $K_3$ was finally fine tuned manually on the nonlinear 6DOF model to have small overshoots. Table 4 shows the controller gain obtained for different Mach numbers at sea level. A large gain reduction is observed between Mach 2.5 and Mach 0.6 indicating that the closed loop bandwidth and projectile maneuverability decrease with the Mach number.

*Table 4: Controller gain*

| Mach | $K_3$ |
|---|---|
| 2.5 | -0.0713 |
| 2 | -0.0500 |
| 1.5 | -0.0310 |
| 1.1 | -0.0200 |
| 0.95 | -0.0045 |
| 0.9 | -0.0044 |
| 0.6 | -0.0036 |

## 4.2 Projectile guidance

The guidance function serves to achieve an accurate impact. Usual artillery targeting systems for unguided projectiles establish gun's azimuth and elevation position on knowledge of muzzle velocity, projectile aerodynamics and known environmental conditions, together with some shell trajectory models. The system determines the launch angular position that will produce a ballistic trajectory intersecting the desired aim point. The guidance method proposed aims at tracking this ballistic trajectory. The ballistic trajectory tracking is achieved by comparing, at the current shell $x$ position, the $y$ and $z$ coordinates of the shell against the desired ones along the reference ballistic trajectory. Only some points of the reference ballistic trajectory need to be stored in the CCF computer at launch. These points are interpolated in flight with piecewise cubic splines to generate the complete reference trajectory.

Linear control theory based on decentralized controllers designed with standard loop-shaping techniques was used to develop the projectile guidance function. The architecture of the guidance and control loops is shown in Fig. 5. This is a classical cascade guidance and control architecture, where the control loop (inner loop) set points are the variables manipulated by the guidance loop.

The guidance loop output variables are the shell positions along the $y$ and $z$ axes of the flat earth reference frame. In Fig. 5, it is important to note that the body frame non-spinning reference pitch and yaw rates were added to the control loop set points to not disturb the guidance loop with this known information. This information was added as a function of the shell position along the flat earth reference frame $x$-axis.

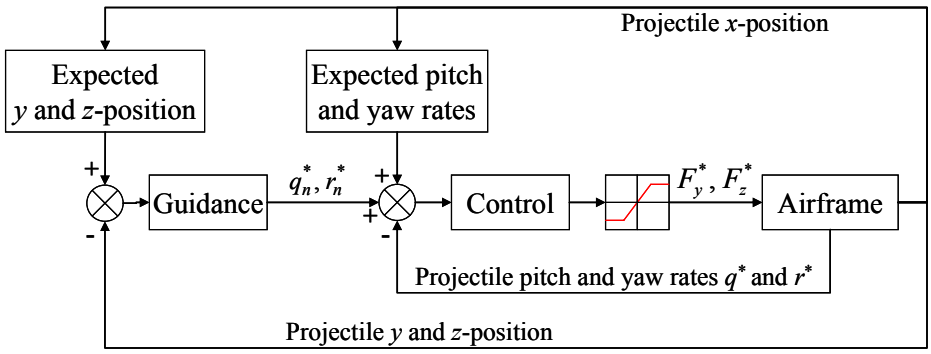


*Figure 5: Guidance and control architecture for the roll-decoupled CCF with four canards*

To select a suitable input-output pairing, temporal simulations were performed for the range of Mach numbers at which the projectile is expected to fly. The pairing $y$ with $r_n^*$ and $z$ with $q_n^*$ appeared clearly the best over the Mach numbers studied. It was necessary to have a linear model between the output variables $y$ and $z$, and the manipulated variables $q_n^*$ and $r_n^*$, to be able to design and tune the decentralized controllers. An output error identification was accomplished to generate the linear model in the body frame non-spinning required. Based on the guidance input-output pairing chosen, the identification was performed only between the output variable $y$ and the manipulated variable $r_n^*$, and between the output $z$ and the manipulated variable $q_n^*$. The transfer functions used for the linear model are shown in Eq. (10). The transfer function parameters identified for different Mach numbers at sea level are listed in Table 5.

$$\frac{y(s)}{r_n^*(s)} = -\frac{z(s)}{q_n^*(s)} = \frac{K_4 e^{-D_1 s}}{(T_1 s+1)s^2} \tag{10}$$

The linear model having two integrators, no additional integrator was required in the decentralized controllers to eliminate potential static errors. However, these two integrators necessitated two lead-lags in each controller to reach an acceptable phase margin. The proposed decentralized controllers are:

$$C_y(s) = -C_z(s) = \frac{K_5(T_2 s+1)(T_2 s+1)}{(0.01T_2 s+1)(0.01T_2 s+1)} \tag{11}$$

For each controller, the gain and lead-lags were tuned initially to obtain the smaller bandwidth that produces a phase margin of 60°. Each controller was finally fine tuned manually on the nonlinear 6DOF model to have small overshoots. Table 6 summarizes the controller parameters after fine tuning for different Mach numbers at sea level. Here, a very large controller gain

reduction is observed between Mach 2.5 and Mach 0.6, indicating that the closed loop bandwidth and projectile maneuverability both decrease with Mach number.

*Table 5: Linear model parameters*

| Mach | $K_4$ | $T_1$ | $D_1$ |
|---|---|---|---|
| 2.5 | 819 | 1.5 | 0 |
| 2 | 657 | 2 | 0 |
| 1.5 | 494 | 3 | 0 |
| 1.1 | 459 | 7 | 0 |
| 0.95 | 460 | 10 | 3 |
| 0.9 | 460 | 15 | 3.5 |
| 0.6 | 192 | 30 | 5 |

*Table 6: Controller parameters*

| Mach | $K_5 \times 10^{-3}$ | $T_2$ |
|---|---|---|
| 2.5 | 1.1000 | 2.2 |
| 2 | 0.7500 | 3.0 |
| 1.5 | 0.2500 | 6.0 |
| 1.1 | 0.0600 | 14 |
| 0.95 | 0.0130 | 40 |
| 0.9 | 0.0110 | 42 |
| 0.6 | 0.0034 | 75 |

# 5 CCF with a drag brake

The objective of this concept is to reduce the delivery error along the longitudinal axis. Current CCF drag brake concepts use drag brakes which are fully deployed at once, without the option to later retract or modulate their positions. The CCF drag brake concept proposed here considers a closed loop control of the drag brake actuator. Hence, the brake-induced drag can be increased or decreased in flight to minimize the miss distance. This concept considers a high update rate of the drag brake amplitude rather than some sporadic changes. The use of a drag brake in closed loop is expected to provide more accuracy.

In the present analysis, the drag brake actuator was not modeled in detail; rather, an external dynamic force was determined and applied on the guided projectile nose along the body frame *x*-axis. The aerodynamics of the guided and unguided projectiles were considered identical. It was also assumed that sensors are available onboard the CCF to measure accurately the projectile states required by the guidance and control functions.

## 5.1 Projectile control

The proposed control strategy consists in computing the velocity profile over the reference ballistic trajectory based on the gun's elevation, muzzle velocity, projectile aerodynamics and known environmental conditions, and to track this reference velocity when the round is in flight. In the present analysis, the velocity tracking was accomplished by comparing the real and reference velocities as a function of time elapsed since launch, but the comparison could also be done as a function of the shell position along the flat earth reference frame *x*-axis. The velocity profile over the reference ballistic trajectory was sampled at a small set of points at launch and was computed in flight using piecewise cubic spline interpolations. The projectile control function was achieved with a linear controller tuned on the linear model between the projectile velocity $V$ and control force $F_x$, which was obtained from the linear 6DOF model of the projectile presented in Chapter 3. Assuming that $\dot{V} \approx \dot{u}$ in Eq. (4), it is possible to write the linear model between $V$ and $F_x$ using the Laplace transform as:

$$\frac{V(s)}{F_x(s)} = \frac{1}{ms} \tag{12}$$

This model is not a function of the Mach number, which means that no gain scheduling for the control function is required. The constant gain controller $C_V(s)$ was used and the projectile mass was included as a separate parameter to facilitate the controller tuning:

$$C_V(s) = mK_6 \tag{13}$$

where $1/K_6$ is the time constant of the closed loop. A time constant of 4 seconds was chosen for the present analysis, which means that the parameter $K_6$ was set at 0.25.

## 5.2 Projectile guidance

The previous control function will improve delivery accuracy along the longitudinal axis by tracking the reference velocity profile, but it cannot manage the projectile position in flight. A guidance function was therefore designed and tuned for this purpose. The proposed guidance strategy tracks the distance traveled along the reference ballistic trajectory as a function of time elapsed since launch. The tracking could also be done as a function of the shell position along the flat earth reference frame *x*-axis. This reference distance profile is computed from the reference ballistic trajectory, based on the gun's elevation, muzzle velocity, projectile aerodynamics and known environmental conditions. It is sampled at a few points that are to be stored in the CCF computer at launch. The reference distance between these points is obtained in flight with piecewise cubic spline interpolations. The projectile guidance function was achieved with a linear controller. The projectile velocity which is the set point of the control loop was chosen as the manipulated variable, producing the cascade guidance and control architecture shown in Fig. 6. In this architecture, the reference velocity was added to the control loop set point to not disturb the guidance loop with this known information.

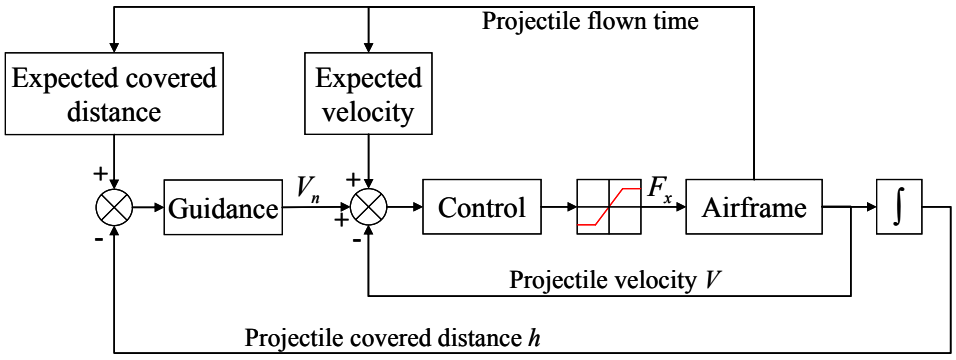


*Figure 6: Guidance and control architecture for the CCF concept with a drag brake*

The relation between the distance covered by the projectile in flight $h$ and the projectile velocity $V$ can be written using the Laplace transform as:

$$\frac{h(s)}{V(s)} = \frac{1}{s} \tag{14}$$

Hence, based on Eqs. (12), (13) and (14), the transfer function between the distance covered by the projectile in flight $h$ and the variable manipulated by the guidance function $V_n$ is:

$$\frac{h(s)}{V_n(s)} = \frac{1}{\left(1 + \frac{s}{K_6}\right)s} \tag{15}$$

This model does not depend on the Mach number, which means that the guidance function will not require gain scheduling. Setting by design that the outer loop will be dynamically 5 times

slower than the inner loop, the time constant in Eq. (15) can be neglected and the following transfer function can be used to design and tune the guidance function:

$$\frac{h(s)}{V_n(s)} = \frac{1}{s} \tag{16}$$

This integrator necessitates only a constant gain controller. Thus, the controller for this model can be written as:

$$C_h(s) = K_7 \tag{17}$$

where $1/K_7$ is the time constant of the closed loop. A time constant of 20 seconds (5 times slower than the inner loop) was chosen for the present analysis, which means that the parameter $K_7$ was set at 0.05.

# 6 CCF with a spin brake

The objective of a spin brake is to manage the projectile drift by modifying its roll rate. This should contribute to a better delivery accuracy along the lateral axis. Only one CCF spin brake concept was found in the literature [8]. This concept uses a spin brake which can be full deployed once without the possibility to retract or modulate its position, so the deploying moment of this spin brake is critical. A more flexible solution to manage the projectile drift would be to use a CCF with a spin brake actuator controlled in closed loop, hence allowing for an increase or decrease of the spin brake amplitude in flight. The concept proposed here considers high update rate corrections applied on the spin brake actuator, which will bring specific challenges for its implementation and requires further investigation.

In the present analysis, the spin brake actuator was not modeled in detail; rather, an external dynamic force was determined and applied on the guided projectile nose to generate a moment which modifies the projectile roll rate. This external control force was applied in the body frame coordinate system at a distance $d/2$ from the projectile centerline. Only the moment generated by this force along the body frame $x$-axis was used. Note that the present analysis assumes that sensors are available onboard the CCF to measure accurately the projectile states required by the guidance and control functions developed.

## 6.1 Projectile control

The projectile roll rate and velocity at the muzzle of the gun are directly proportional. As a result, the roll rate can vary slightly from round to round. During its flight, it is important to control the projectile roll rate to obtain an accurate projectile drift. In the present analysis, a closed loop control was designed and tuned on the projectile roll rate. The control strategy aims at tracking the roll rate profile of the projectile along the reference ballistic trajectory leading to the aim point. The reference roll rate profile was tracked as a function of time elapsed since launch, but could also be tracked as a function of the shell position along the flat earth reference frame $x$-axis. The reference profile was again computed on the basis of the gun's elevation, muzzle velocity, projectile aerodynamics and known environmental conditions. Only a sample of points needs be stored in the CCF computer at launch. These points are interpolated in flight with piecewise cubic splines to generate the complete reference profile. A linear controller, designed and tuned with the linear model between the projectile roll rate $p$ and control force $F_s$, was used to track the reference roll rate profile when the round was flying. The linear model between the projectile roll rate $p$ and control force $F_s$ was obtained from the linear 6DOF model of the projectile presented in Chapter 3. Based on Eq. (3) and using the Laplace transform, the model can be written as:

$$\frac{p(s)}{F_s(s)} = \frac{d}{2I_x s} \tag{18}$$

This model does not depend on the Mach number, which means that no gain scheduling for the control function is required. The linear controller used is:

$$C_p(s) = \frac{2I_x K_8}{d} \tag{19}$$

where $1/K_8$ is the time constant of the closed loop. A time constant of 4 seconds was chosen for the present analysis, which means that the parameter $K_8$ was set at 0.25.

## 6.2 Projectile guidance

The above closed loop control on the projectile roll rate will contribute to improve delivery accuracy along the lateral axis, but this function will not manage the lateral position of the projectile in flight. Hence, a guidance function was designed and tuned for this purpose.

The proposed guidance strategy aims at tracking the reference lateral position of the shell as a function of its position along the flat earth reference frame $x$-axis. The reference position profile is computed based on the gun's azimuth and elevation, muzzle velocity, projectile aerodynamics and known environmental conditions. It is sampled at some points, which are to be stored in the CCF computer at launch. These points are interpolated in flight with piecewise cubic splines to generate the reference position required. The set point of the control loop on the projectile roll rate was used as the manipulated variable of the guidance loop, creating the cascade guidance and control architecture shown in Fig. 7. In this architecture, the reference roll rate was added to the control loop set point to not disturb the guidance loop with this known information. A linear controller was used to execute the guidance function. Therefore, a linear model was generated between the projectile lateral position $y$ and the variable manipulated by the guidance function $p_n$.

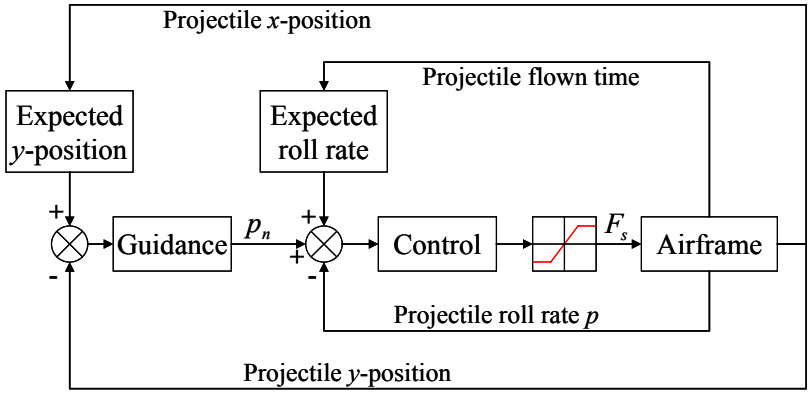


*Figure 7: Guidance and control architecture for the CCF concept with a spin brake*

The projectile yaw of repose $\beta_r$ can be calculated from:

$$QSdC_{m\alpha}\beta_r + \frac{I_x pg\cos\theta}{V} = 0 \tag{20}$$

With the following approximations:

$$\beta_r \approx -\frac{v}{V} \approx -\frac{\dot{y}}{V} \tag{21}$$

it is possible to write:

$$-\frac{QSdC_{m\alpha}\dot{y}}{V} + \frac{I_x pg\cos\theta}{V} = 0 \tag{22}$$

Assuming that the outer loop is dynamically slower than the inner loop by a factor of 5, the transfer function between the projectile lateral position $y$ and the variable manipulated by the guidance function $p_n$ can be written as:

$$\frac{y(s)}{p_n(s)} = \frac{I_x g\cos\theta}{QSdC_{m\alpha}s} \tag{23}$$

This linear model being an integrator, the constant gain controller $C_y(s)$ was used in the present analysis:

$$C_y(s) = \frac{QSdC_{m\alpha}K_9}{I_x g\cos\theta} \tag{24}$$

where $1/K_9$ is the time constant of the closed loop. A time constant of 20 seconds (5 times slower than the inner loop) was chosen for the present analysis, which means that the parameter $K_9$ was set at 0.05.

# 7 Simulation results and analysis

The performance of the different CCF concepts and the guidance and control algorithms described previously were verified using Monte Carlo simulations with the nonlinear 6DOF model of the projectile. Perturbations were applied on the muzzle velocity, gun's azimuth and elevation, and longitudinal and lateral wind velocity. A Monte Carlo run consisted in flying the shell 200 times with particular standard deviations on the perturbations under study. Hence, the perturbations were varied randomly from round to round according to separate normal distributions. The standard deviations applied in this analysis are summarized in Table 7.

*Table 7: Perturbation standard deviations*

| Perturbation | Standard deviation |
|---|---|
| Muzzle velocity | 2 m/s |
| Gun's azimuth and elevation | 0.5 mil |
| Longitudinal and lateral wind velocity in the flat earth reference frame | 2 m/s |

These standard deviations were considered appropriate and conservative. Standard deviations of 2 m/s on gun muzzle velocity were observed on some actual systems. A standard deviation of 0.5 mil on the gun's azimuth and elevation was chosen based on the operational characteristics of typical current gun aiming systems. Finally, a standard deviation of 2 m/s on the longitudinal and lateral wind velocity, relative to the expected conditions, was also considered realistic.

All rounds were launched with the same nominal conditions: muzzle velocity of 823 m/s, nil longitudinal and lateral wind velocity, and gun's azimuth and elevation of 0° and 45° respectively. Thus, the aim point position and projectile reference behaviour were the same for all simulations. Guidance and control gain scheduling were used to take into account the projectile's airspeed variation for the roll-decoupled four canard concept. The sea level dynamic pressure was used over the entire flight in all runs in order to simplify the analysis, by eliminating the need to implement gain scheduling as a function of the altitude, for all CCF concepts. The effect of altitude will be verified in follow-on work.

The longitudinal and lateral components of the delivery accuracy, measured as probable error (PE), were used to quantify the accuracy obtained with each CCF concept. From the definition of PE, the probability of a round falling within a zone extending one PE on either side of the mean point of impact is 50%, attention being confined to deviation along one axis [32]. For a normal distribution, which was assumed in the present analysis, the longitudinal and lateral PE components ($E_x$, $E_y$) are obtained, respectively, as:

$$E_x = 0.67449\sigma_x^*$$
$$E_y = 0.67449\sigma_y^* \tag{25}$$

where $\sigma_x$* and $\sigma_y$* are the longitudinal and lateral standard deviations of the dispersion pattern at impact. The longitudinal and lateral standard deviations are computed using the standard deviations along the $x$ and $y$ axes of the flat earth reference frame and the rotation angle $\lambda$ of the dispersion pattern as:

$$\sigma_x^* = \sqrt{\left(\sigma_x^2 \cos^2 \lambda - \sigma_y^2 \sin^2 \lambda\right) \sec 2\lambda}$$
$$\sigma_y^* = \sqrt{\left(-\sigma_x^2 \sin^2 \lambda + \sigma_y^2 \cos^2 \lambda\right) \sec 2\lambda} \tag{26}$$

where the angle $\lambda$ is computed as:

$$\lambda = 0.5 \arctan \frac{2\rho\sigma_x\sigma_y}{\sigma_x^2 - \sigma_y^2} \tag{27}$$

The variable $\rho$ represents the correlation coefficient between the deviations $\Delta x$ and $\Delta y$ in the flat earth reference frame.

In the next three sections (7.1, 7.2 and 7.3), Figs. 8, 10 and 12 show the miss distances achieved with different actuator saturation limits as a function of the perturbations studied. Each individual graph on a figure shows a Monte Carlo run with 200 simulations. On each figure, the first column presents the Monte Carlo trials for the case with no guidance and control applied (±0 N (Newton) saturation limits on the actuator(s)), and the last column shows the results without a saturation limit on the actuator(s). The second and third columns illustrate the performance obtained for the actuator saturation limits indicated. On each figure, the first row is for a standard deviation of 2 m/s applied to the muzzle velocity, the second row, for a standard deviation of 0.5 mil on the gun's azimuth and elevation, the third row, for a standard deviation of 2 m/s on the longitudinal and lateral wind velocity, and the last row, is where all perturbations of Table 7 are applied simultaneously.

Figures 9, 11 and 13 show the longitudinal and lateral PE using red and blue lines, respectively, for the muzzle velocity, gun's azimuth and elevation, longitudinal and lateral wind and all standard deviation(s) of Table 7. The longitudinal and lateral PE are presented as a function of the actuator saturation limits. The positive horizontal axis on each graph implicitly assumes that the actuator(s) can vary symmetrically across the 0 mark with the same amplitude.

## 7.1 Roll-decoupled CCF with canards

This section discusses the results obtained with the concept of a roll-decoupled CCF controlling four canards. The results without guidance and control, first column in Fig. 8, show that the wind velocity perturbations have the larger effect on the projectile accuracy. Figure 8 also shows that this CCF concept can improve greatly the projectile accuracy against gun's azimuth and elevation perturbations (second row of Fig. 8). This CCF concept is not effective against muzzle velocity and longitudinal wind perturbations (first and third rows of Fig. 8), but it reduces significantly the

effect of lateral wind perturbations (third row of Fig. 8). A comparison of the third and last rows of Fig. 8 shows that the overall accuracy is driven by the perturbations having the larger effect on the projectile, namely, the wind velocity perturbations in the present analysis. Also, a comparison of the second and third columns with the last one indicates that saturation limits between ±10 N and ±20 N yield nearly optimal performance. This is better illustrated in Fig. 9, where the bottom left and top right graphics show that a very low force is required to obtain nearly optimal results when lateral wind or gun's azimuth and elevation perturbations are present. Actuator saturation limits of ±10 N are suggested by these results. The top left and bottom left graphics of Fig. 9 confirm that a roll-decoupled CCF controlling four canards has no significant effect on muzzle velocity and longitudinal wind perturbations.

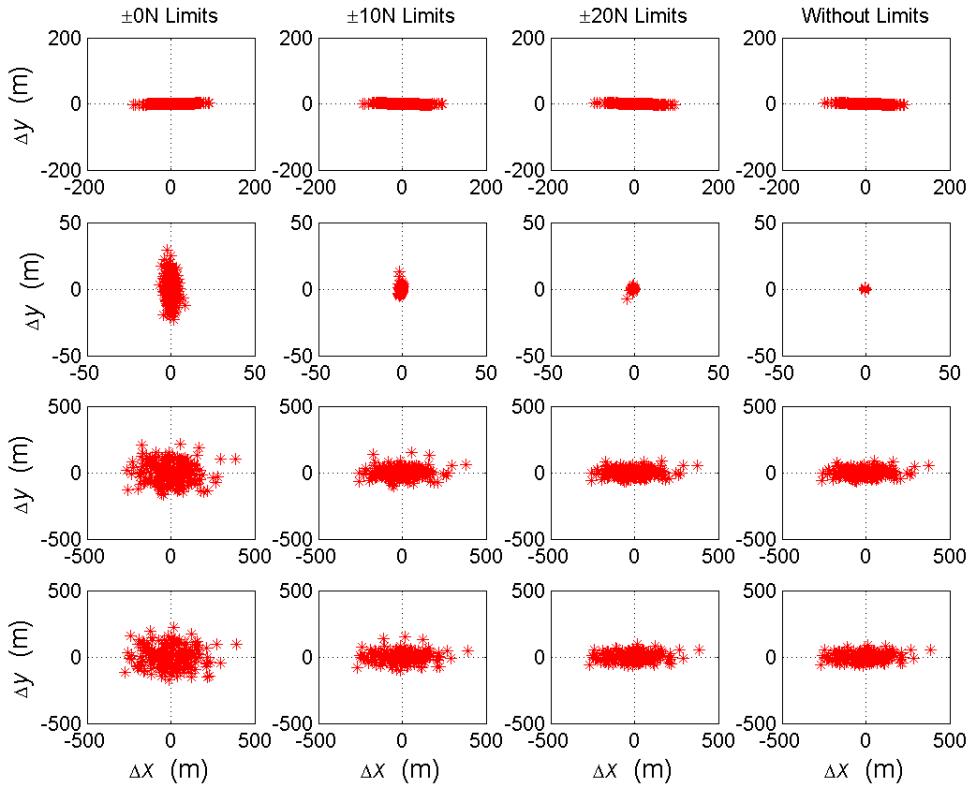


*Figure 8: Miss distances of the roll-decoupled CCF with canards (first row: muzzle velocity effect; second row: gun's orientation effect; third row: wind velocity effect; fourth row: all)*

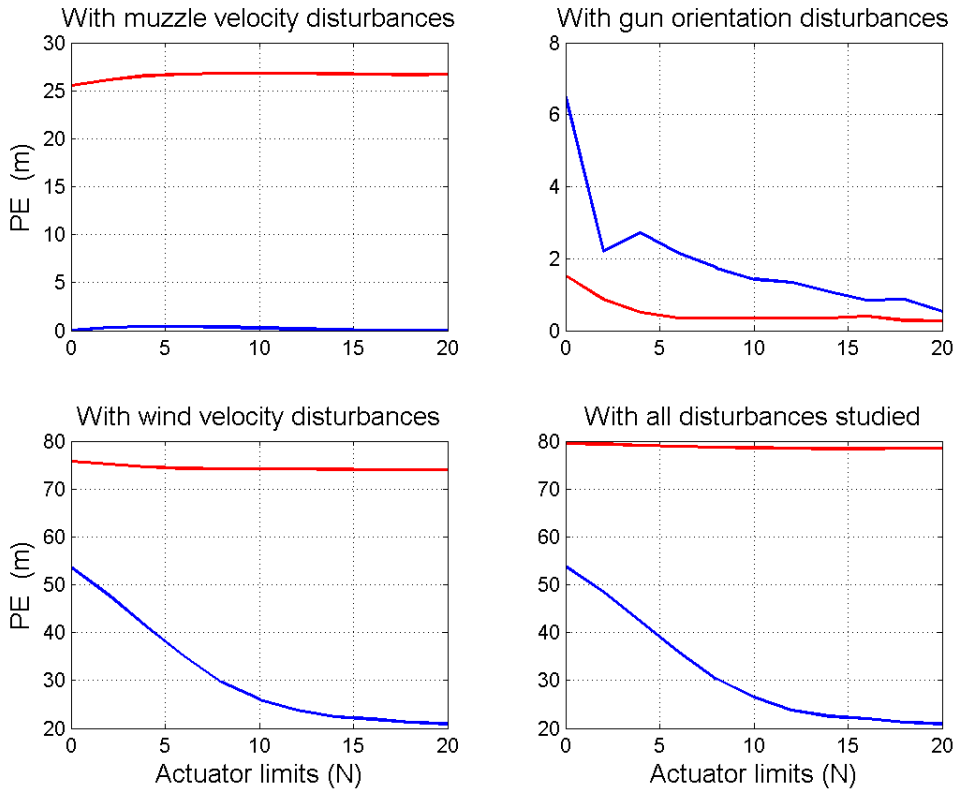


*Figure 9: Probable errors as a function of the actuator saturation limits for the roll-decoupled CCF with canards (—— longitudinal PE, —— lateral PE)*

## 7.2 CCF with a drag brake

This section discusses the results obtained with the drag brake CCF concept proposed. The second column of Fig. 10 indicates that a drag brake actuator, which can vary from -10 N to 0 N, may correct one side of the longitudinal axis only. Positive and negative forces are required to reduce the miss distances along both side of the longitudinal axis, as shown in the third column of Fig. 10. No accuracy deterioration is observed along the lateral axis, because the drag brake actuator was assumed ideal. Figure 10 also shows that a drag brake actuator can improve greatly the projectile accuracy in the presence of muzzle velocity or longitudinal wind perturbations. However, this CCF concept increases the miss distances with gun's elevation perturbations. Nevertheless, the accuracy improvement obtained in the presence of muzzle velocity or longitudinal wind perturbations is the dominating element. A comparison of the third column with the last one shows that a low drag force is sufficient to obtain a nearly optimal performance. This is also illustrated in Fig. 11 where the top left graph shows that a very low drag force is sufficient to alleviate the impact of muzzle velocity perturbations. The drag force required to fight against the longitudinal wind perturbations is more important, as shown by the bottom left graphic of Fig. 11. However, actuator saturation limits of ±10 N seem sufficient to obtain results

which are close to the best ones observed in the figure. From the top right graph of Fig. 11, the longitudinal PE for the gun's elevation perturbations remain constant for non-zero actuator saturation limits, which will be investigated further in follow-on work. As expected, Fig. 11 shows clearly that this CCF concept has no significant effect on the projectile lateral accuracy.

Two operational applications seem possible with the concept proposed. A long range application where the projectile would be launched with its drag brake amplitude at zero on a reference ballistic trajectory calculated without any drag brake. In this application, the drag brake actuator would be able to decrease the projectile range, but would not be able to increase it. This application could be of value to limit potential collateral damage behind the aim point. Another operational application would be to launch the projectile with its drag brake amplitude at 50% on a reference ballistic trajectory calculated for a 50% constant drag brake amplitude. Here, the drag brake actuator would be able to increase or decrease the projectile range. However, the maximum range for this application would be shorter than the maximum unguided projectile range.

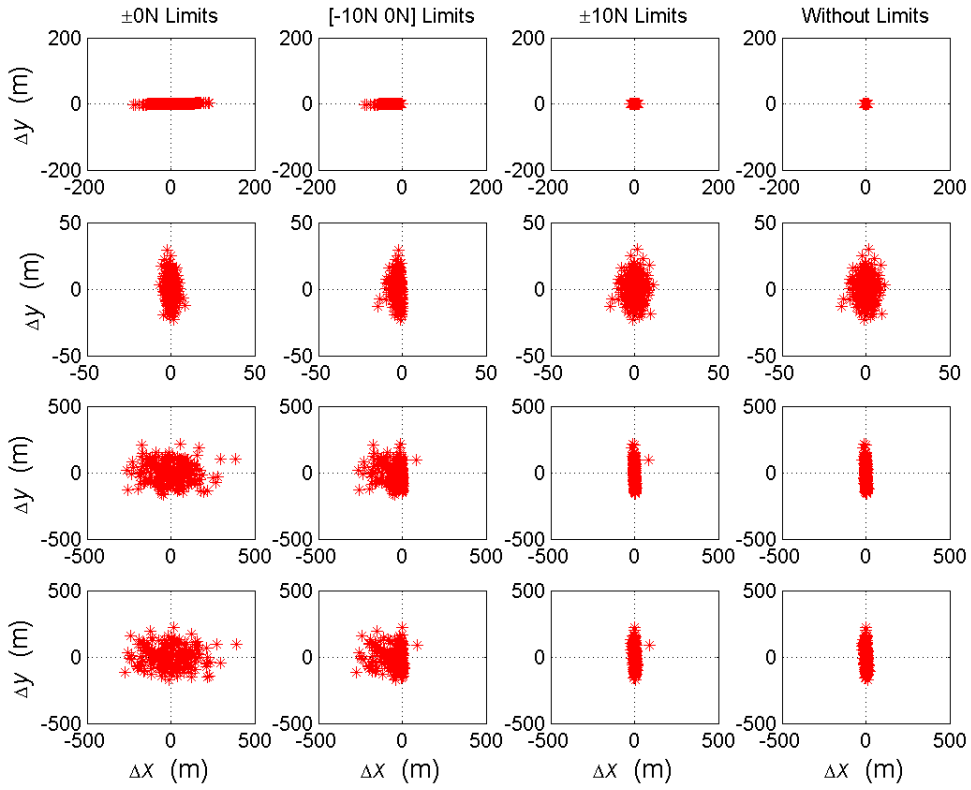


*Figure 10: Miss distances of the proposed CCF with a drag brake (first row: muzzle velocity effect; second row: gun's orientation effect; third row: wind velocity effect; fourth row: all)*

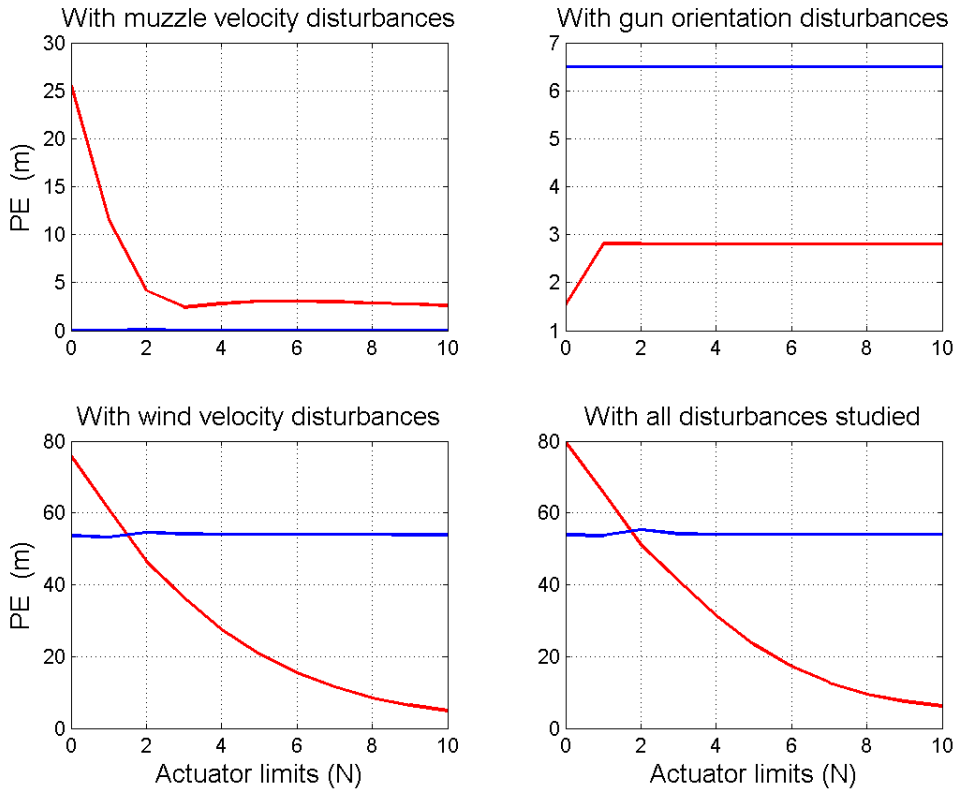


*Figure 11: Probable errors as a function of the actuator saturation limits for the proposed CCF with a drag brake (—— longitudinal PE, —— lateral PE)*

## 7.3 CCF with a spin brake

This section discusses the results obtained with the spin brake CCF concept proposed. In Fig. 12, a comparison of the second column with the third one shows that positive and negative actuator forces are required to control the projectile accuracy on both sides of the lateral axis. No accuracy degradation is observed along the longitudinal axis, because the spin brake actuator was assumed ideal, which means that no drag is generated by this actuator. Figure 12 shows that the proposed concept can improve greatly the projectile accuracy when gun's azimuth or lateral wind perturbations are present, as shown in the second and third rows of Fig. 12. From the third and fourth columns, actuator saturation limits of ±26 N yield a nearly optimal performance. This is better illustrated in Fig. 13, where the top right graph shows that a very low force is sufficient to reduce significantly the effect of gun's azimuth perturbations. The lateral PE curve further indicates that actuator saturation limits of ±2 N yield a similar lateral accuracy as actuator saturation limits of ±25 N, while a choice in between produces a larger lateral PE. The force required to compensate for the lateral wind perturbations is much higher, as shown by the bottom left graph of Fig. 13. Nevertheless, saturation limits of ±26 N are sufficient to improve noticeably the projectile delivery accuracy. The top left graph of Fig. 13 shows that the spin brake does not

correct muzzle velocity perturbations, which means that this actuator type is not suitable for these perturbations. As expected, Fig. 13 shows that the ideal spin brake actuator used here, which generates no drag, has no effect on the projectile longitudinal accuracy. A real spin brake actuator will produce some drag, which should impact on the projectile longitudinal accuracy and range.

Two operational applications could be possible with the concept proposed. A long range application where the projectile would be launched with its spin brake amplitude at zero on a reference ballistic trajectory calculated without any spin brake. In this application, the spin brake actuator would be able to decrease the projectile drift but not able to increase it. This application could be interesting to limit potential collateral damage at a higher drift variation than the lateral aim point position. Another operational application would be to launch the projectile with its spin brake amplitude at 50% on a reference ballistic trajectory calculated for a 50% constant spin brake amplitude. Here, the spin brake actuator would be able to increase or decrease the projectile drift to reduce the miss distance along the lateral axis. In this application, however, the maximum range would be shorter than the maximum unguided projectile range.

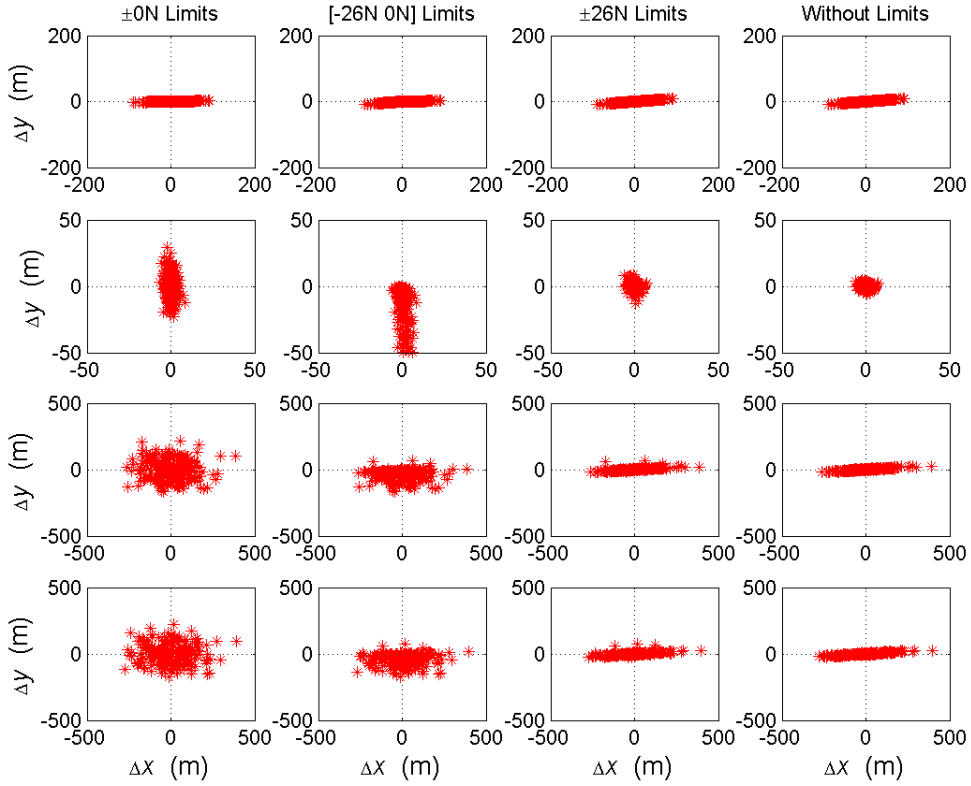


*Figure 12: Miss distances of the proposed CCF with a spin brake (first row: muzzle velocity effect; second row: gun's orientation effect; third row: wind velocity effect; fourth row: all)*

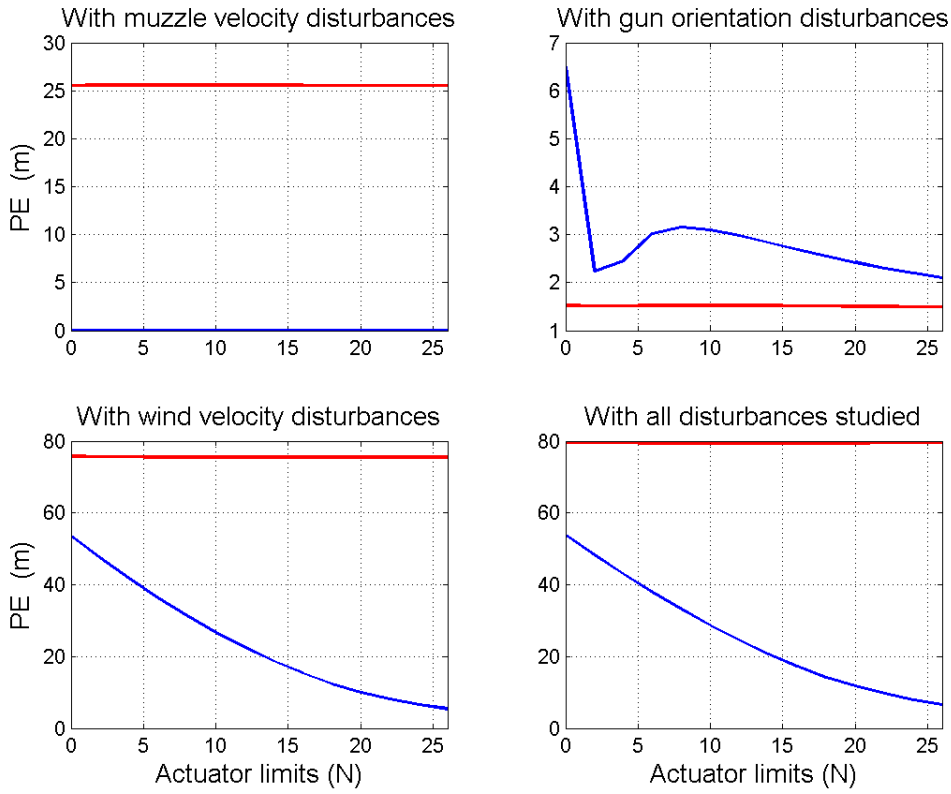


*Figure 13: Probable errors as a function of the actuator saturation limits for the proposed CCF with a spin brake (—— longitudinal PE, —— lateral PE)*

## 7.4 CCF comparison

This section compares a 2DOF CCF concept, made of both the drag brake and spin brake concepts proposed, against the four canard one. Figure 14 shows the miss distances achieved without actuator saturation limit for the various perturbations. Each graph on Fig. 14 shows again a Monte Carlo run with 200 simulations. The first column of Fig. 14 corresponds to the case without guidance and control. The second column shows the simulation results when the drag brake and spin brake concepts proposed are used simultaneously to improve the longitudinal and lateral accuracy, while the third column presents the miss distances achieved with the four canard concept. The last column shows the four canard concept with the addition of the drag brake concept proposed. This custom concept generates independent corrections along the *x*, *y* and *z* axes. The first, second, third and last rows of Fig. 14 show, respectively, the Monte Carlo runs in the presence of muzzle velocity, gun's azimuth and elevation, longitudinal and lateral wind and all perturbations, using again the standard deviations of Table 7.

The second column of Fig. 14 shows that the combined drag-spin brake concept performs very well to reduce muzzle velocity and wind perturbation effects. The four canard concept (third

column of Fig. 14) does better against the gun's azimuth and elevation perturbations, but these perturbations have a smaller effect on the projectile than the other perturbations. Overall, the results shown in the last row of Fig. 14 favour largely the combined drag-spin brake concept. In the last column of Fig. 14, the addition of a drag brake to the four canard concept improves greatly its performance along the longitudinal axis, but overall, it does not perform as well as the combined drag-spin brake concept.

Table 8 summarizes all longitudinal and lateral PE results presented so far for the case without actuator limit, for all CCF concepts studied.

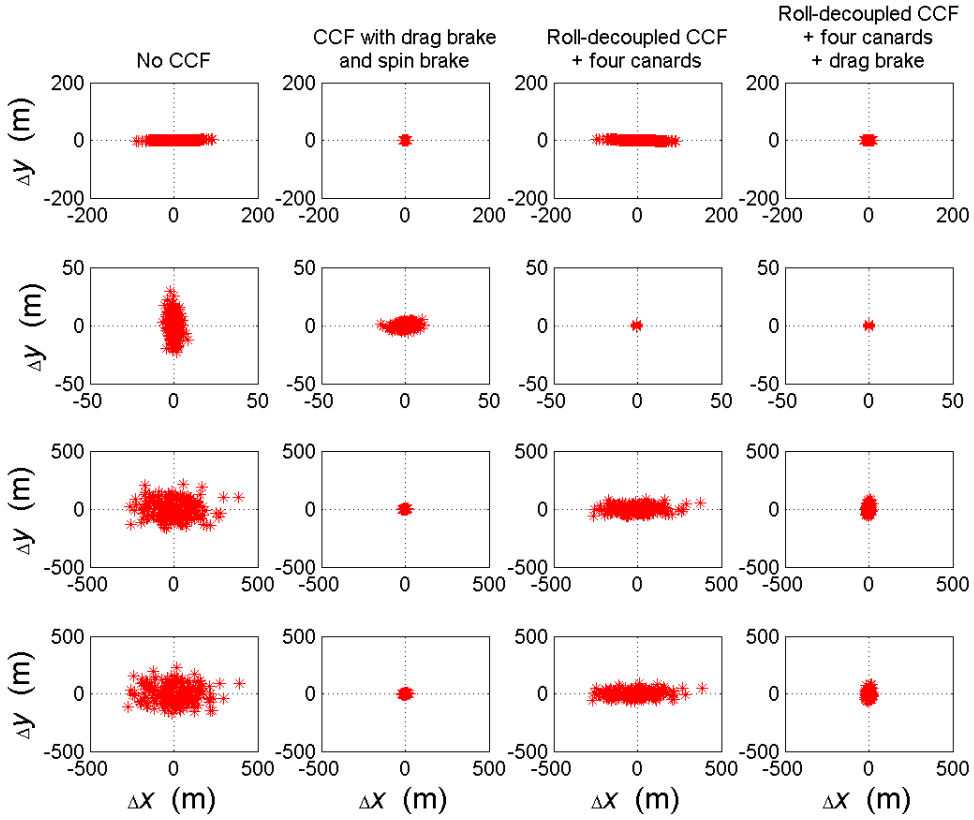


*Figure 14: Miss distances of different CCF concepts (first row: muzzle velocity effect; second row: gun's orientation effect; third row: wind velocity effect; fourth row: all)*

*Table 8: PE of the CCF concepts studied without actuator saturation limit (longitudinal PE (m) above, lateral PE (m) below, on each row)*

| Longitudinal PE (m)<br>Lateral PE (m) | Muzzle velocity perturbations | Gun's azimuth and elevation perturbations | Longitudinal and lateral wind perturbations | All perturbations |
|---|---|---|---|---|
| No CCF | 25.53<br>0.0001 | 1.53<br>6.50 | 75.79<br>53.64 | 79.56<br>53.84 |
| CCF with drag brake | 1.65<br>0.0001 | 2.81<br>6.50 | 3.04<br>53.94 | 4.41<br>53.96 |
| CCF with spin brake | 25.57<br>0.008 | 1.65<br>1.25 | 75.55<br>1.86 | 79.49<br>2.26 |
| CCF with drag brake and spin brake | 1.65<br>0.0001 | 2.85<br>1.33 | 4.04<br>1.53 | 5.10<br>2.07 |
| Roll-decoupled CCF + four canards | 26.82<br>0.04 | 0.05<br>0.23 | 73.96<br>20.57 | 78.33<br>20.53 |
| Roll-decoupled CCF + four canards + drag brake | 3.36<br>0.0005 | 0.02<br>0.23 | 4.67<br>20.57 | 5.78<br>20.57 |

# 8 Conclusions and recommendations

Future artillery systems will require guided projectiles for accuracy. This report summarized an analysis on course correction fuze (CCF) options to guide in-service conventional indirect fire spin-stabilized projectiles. CCF concepts using a drag brake, a spin brake and a four canard configuration, were studied. A typical 155 mm spin-stabilized gunnery shell was selected for the analysis.

Both linear and nonlinear 6DOF models of the projectile were formulated to design and tune the controllers for both guidance and control functions, and to analyze both guided and non-guided projectiles. Guidance and control functions were designed to track the reference ballistic trajectory, and implemented in inner and outer loops within cascade architectures. Using this approach, the current operational firing tables providing impact data as a function of muzzle velocity, launch angle and known environmental conditions can be used. The proposed approach uses table look up and interpolation, and therefore requires relatively low computing power, compared with methods using recursive predictions of the remaining flight trajectory. Finally, tracking the projectile reference ballistic trajectory means relatively low guidance corrections, hence low induced drag and better airspeed.

The performance of the CCF concepts were analyzed through Monte Carlo simulations as a function of perturbations in muzzle velocity, gun's azimuth and elevation, and longitudinal and lateral wind velocity. The drag brake concept was found to be highly capable of compensating perturbations in muzzle velocity and longitudinal wind velocity. The spin brake concept compensated for lateral wind perturbations and reduced significantly the gun's azimuth perturbation effect. The four canard concept compensated for the gun's azimuth and elevation perturbations efficiently. Based on the perturbation standard deviations used, the muzzle velocity and wind velocity perturbations were found to have a higher effect on the projectile dispersion at impact than the gun's azimuth and elevation perturbations. A CCF combining the drag and spin brakes was therefore proposed, and found to be a better overall choice than the four canard configuration.

In summary, the proposed CCF concepts showed potential for course correction. Further work is recommended to include realistic CCF actuator systems for drag and roll rate control. The aerodynamic tables should also include the presence of these actuators; hence induced drag would be produced when the actuators are operated. Along with these more detailed concepts, the dynamic pressure variation as a function of the altitude, and the projectile Magnus moment would be considered. Also, particular guidance and control algorithms could be studied, such as the multivariable guidance and control with decouplers to reject the coupling between the actuators without increasing computing power requirements. A similar CCF comparative analysis could also be performed on other smaller spin-stabilized projectiles. Finally, the effectiveness of the CCF concepts to meet objective delivery accuracy is a function of the sensors used to measure the projectile states. Further work is thus recommended to establish sensor requirements to achieve the desired performance.

# References


[1] Giat Industries, *SPACIDO Le tir d'artillerie de précision (1)*. Advertising data from Giat Industries, www.giat-industries.fr

[2] Reusch O. and Kautzsch K.B. (2003). Precision Enhancement build on a Multi Functional Fuze for 155 mm Artillery Munition. *NDIA 47th NDIA Annual Fuze Conference*.

[3] Beattie R. (2000). UK Course Correction Fuze Research. 6th International Cannon Artillery Firepower Symposium & Exhibition.

[4] D'Amico W.P.Jr. (1996). Low Cost Competent Munitions Program. *Test Technology Symposium '96*.

[5] Hollis M.S.L. (1996). Preliminary Design of a Range Correction Module for an Artillery Shell. *US Army Research Laboratory*, Aberdeen Proving Ground, MD, ARL-MR-298 Report, 17 p.

[6] Hollis M.J.L. and Brandon F.J. (1999). Design and Analysis of a Fuze-Configurable Range Correction Device for an Artillery Projectile. *US Army Research Laboratory*, Aberdeen Proving Ground, MD, ARL-TR-2074 Report, 71 p.

[7] Finch C. and Werko R. (2004). Guidance Integrated Fuze (GIF) / Course Correction Fuze (CCF). *NDIA 48th Annual Fuze Conference*.

[8] Hillstrom T. and Osborne P. (2005). United Defense Course Correcting Fuze for the Projectile Guidance Kit Program. NDIA 49th Annual Fuze Conference.

[9] Regan F.J. and Smith J. (1975). Aeroballistics of a Terminally Corrected Spinning Projectile (TCSP). *Journal of Spacecraft*, *12*(12), 733-740.

[10] Dietrich S., Rainville P.A. and Tran L.B. (2006). Guided Artillery Projectiles Study. *DRDC Valcartier contractor report*, from SNC TEC company, CR 2006-002.

[11] Parisé N. (2005). Trajectory Correction Fuzes for Conventional Artillery Ammunition. *DRDC Valcartier contractor report*, from SNC TEC company, CR 2005-319.

[12] Gagnon E. (2007). Controllability study of the 155 mm projectile. *DRDC Valcartier technical report*, Defence R&D Canada - Valcartier, TR 2006-734.

[13] Gagnon E. and Lauzon M. (2007). Maneuverability Analysis of the Conventional 155 mm Gunnery Projectile. *AIAA Guidance, Navigation, and Control Conference & Exhibit*, AIAA Paper 2007-6784, August 20-23, Hilton Head, South Carolina.

[14] Pamadi K.B. and Ohlmeyer E.J. (2006). Evaluation of Two Guidance Laws for Controlling the Impact Flight Path Angle of a Naval Gun Launched Spinning Projectile. *AIAA Guidance, Navigation, and Control Conference & Exhibit*, AIAA Paper 2006-6081, August 21-24, Keystone, Colorado.

[15] Ollerenshaw D. and Costello M. (2005). Model Predictive Control of a Direct Fire Projectile Equipped with Canards. *AIAA Atmospheric Flight Mechanics Conference and Exhibit*, AIAA paper 2005-5818, August 15-18, San Francisco, California.

[16] Costello M.F. (1997). Potential Field Artillery Projectile Improvement Using Movable Canards. *US Army Research Laboratory*, Aberdeen Proving Ground, MD, ARL-TR-1344 Report, 52 p.

[17] Hainz III L.C. and Costello M. (2005). Modified Projectile Linear Theory for Rapid Trajectory Prediction. *Journal of Guidance, Control and Dynamics*, *28*(5), 1006-1014.

[18] Burchett B. and Costello M. (2002). Model Predictive Lateral Pulse Jet Control of an Atmospheric Rocket. *Journal of Guidance, Control and Dynamics*, *25*(5), 860-867.

[19] Slegers N. (2007). Model Predictive Control of a Low Speed Munition. *AIAA Atmospheric Flight Mechanics Conference and Exhibit*, AIAA paper 2007-6583, August 20-23, Hilton Head, South Carolina.

[20] Calise A.J. and El-Shirbiny H.A. (2001). An Analysis of Aerodynamic Control for Direct Fire Spinning Projectiles. *AIAA Guidance, Navigation, and Control Conference & Exhibit*, AIAA paper 2001-4217, August 6-9, Montreal, Quebec, Canada.

[21] Calise A.J., El-Shirbiny H.A., Kim N. and Kutay A.T. (2004). An Adaptive Guidance Approach for Spinning Projectiles. *AIAA Guidance, Navigation, and Control Conference & Exhibit*, AIAA paper 2004-5359, August 16-19, Providence, Rhode Island.

[22] Jitpraphai T., Burchett B. and Costello M. (2001). A Comparison of Different Guidance Schemes for a Direct Fire Rocket with a Pulse Jet Control Mechanism, *AIAA Atmospheric Flight Mechanics Conference and Exhibit*, AIAA paper 2001-4326, August 6-9, Montréal, Canada.

[23] Jitpraphai T. and Costello M. (2001). Dispersion Reduction of a Direct Fire Rocket Using Lateral Pulse Jets. *Journal of Spacecraft and Rockets*, *38*(6), 929-936.

[24] Stilley G.D. and Alford R.L. (1984). Axis System Considerations for Guidance and Stability of Spinning Projectiles. 22nd *AIAA Aerospace Sciences Meeting*, AIAA paper 1984-327, January 9-12, Reno, NV.

[25] Blakelock J.H. (1991). Automatic Control of Aircraft and Missiles, Second Edition. John Wiley & Sons, Inc., pp. 14.

[26] McCoy R.L. (1999). Modern Exterior Ballistics, The Launch and Flight Dynamics of Symmetric Projectiles. Atglen, PA: Schiffer Publishing Ltd, pp. 37, pp. 157-164.

[27] Dupuis A.D. (1998). Components of Ballistic Error (Some parameters affecting the flight path of a projectile). *Defence Research & Development Canada*, Valcartier, Québec, Prepared in support of the land force technical staff course, 50 p.

[28] Lloyd K.H. and Brown D.P. (1979). Instability of Spinning Projectiles During Terminal Guidance. *Journal of Guidance and Control*, *2*(1), 65-70.

[29] Ljung L. (1987). *System Identification – Theory for the User*. Prentice Hall, Englewood Cliffs, N.J.

[30] Skogestad S. and Postlethwaite I. (1996). *Multivariable feedback control*. John Wiley & Sons, England.

[31] Maciejowski J.M. (1989). *Multivariable Feedback Design*. Addison-Wesley, England.

[32] Vincent R. (1987). *Textbook of Ballistics and Gunnery, Volume One*. London: Her Majesty's Stationery Office., pp. 470-473.

This page intentionally left blank.

# List of symbols/abbreviations/acronyms/initialisms

| | |
|---|---|
| $\alpha, \beta$ | Body frame angles of attack and sideslip |
| $\dot{\alpha}, \dot{\beta}$ | Rate of change of body frame angles of attack and sideslip |
| $\beta_r$ | Yaw of repose |
| $\theta$ | Euler pitch angle |
| $\lambda$ | Rotation angle of the dispersion pattern at impact, from the flat earth reference frame |
| $\rho$ | Correlation coefficient between the dispersion errors $\Delta x$ and $\Delta y$ at impact |
| $\sigma_x, \sigma_y$ | Standard deviations of the dispersion pattern along the $x$ and $y$ axes of the flat earth reference frame |
| $\sigma_x^*, \sigma_y^*$ | Longitudinal and lateral standard deviations of the dispersion pattern at impact |
| $\omega_1, \omega_2, \omega_3$ | Natural frequencies |
| $\zeta_1, \zeta_2, \zeta_3$ | Damping factors |
| $C_{L\alpha}$ | Non-dimensional lift force coefficient |
| $C_{m\alpha}$ | Non-dimensional overturning moment coefficient |
| $C_{m\dot{\alpha}}$ | Non-dimensional pitch damping moment coefficient due to the rate of change of the attack angle |
| $C_{mP\alpha}$ | Non-dimensional Magnus moment coefficient |
| $C_{mq}$ | Non-dimensional pitch damping moment coefficient due to the pitch rate |
| $d$ | Reference cross-sectional diameter |
| $D_1$ | Delay |
| $C_V, C_h, C_p, C_y, C_z, C_{r^*}, C_{q^*}$ | Controllers |
| $E_x, E_y$ | Longitudinal and lateral probable dispersion errors at impact |
| $F_s$ | Force applied on the projectile nose to change the roll rate |
| $F_x, F_y, F_z$ | Forces applied on the projectile nose along the body frame $x$, $y$ and $z$ axes |
| $F_y^*, F_z^*$ | Forces applied on the projectile nose along the body frame non-spinning $y$ and $z$ axes |
| $g$ | Acceleration due to gravity |
| $h$ | Distance covered by the projectile along its ballistic trajectory |

| | |
|---|---|
| $I_x, I_y, I_z$ | Moments of inertia about the body frame *x*, *y* and *z* axes |
| $K_1, K_2, K_3, K_4, K_5, K_6, K_7, K_8, K_9$ | Guidance and control gains |
| $l$ | Length |
| $m$ | Mass |
| $M_\alpha$ | Dimensional overturning moment coefficient |
| $M_{\dot{\alpha}}$ | Dimensional pitch damping moment coefficient due to the rate of change of the attack angle |
| $M_{P\alpha}$ | Dimensional Magnus moment coefficient |
| $M_q$ | Dimensional pitch damping moment coefficient due to the pitch rate |
| $p_n$ | Roll rate set point |
| $p, q, r$ | Body frame roll, pitch and yaw rates |
| $\dot{p}, \dot{q}, \dot{r}$ | Rate of change of the body frame roll, pitch and yaw rates |
| $q^*, r^*$ | Body frame non-spinning pitch and yaw rates |
| $q_n^*, r_n^*$ | Body frame non-spinning pitch and yaw rate set points |
| $Q$ | Dynamic pressure |
| $s$ | Laplace operator |
| $S$ | Reference cross-sectional area |
| $T_1, T_2$ | Time constants |
| $u, v, w$ | Body frame projectile velocity components |
| $\dot{u}, \dot{v}, \dot{w}$ | Rate of change of the body frame projectile velocity components |
| $V$ | Projectile velocity |
| $V_n$ | Projectile velocity set point |
| $x, y, z$ | Airframe position in the flat earth reference frame |
| $x_{cg}$ | Gravity center position, measured from the nose |
| $\Delta x, \Delta y$ | Miss distance along the *x* and *y* axes of the flat earth reference frame |
| $\dot{y}$ | Rate of change of the lateral airframe position |
| $Z_\alpha$ | Dimensional lift force coefficient |
| 1D | One-Dimensional |
| 2D | Two-Dimensional |

| | |
|---|---|
| 2DOF | Two-Degree-Of-Freedom |
| 6DOF | Six-Degree-Of-Freedom |
| CCF | Course Correction Fuze |
| DATCOM 02 | US AFRL Missile DATCOM aero-prediction tool (Version 2002) |
| DRDC | Defence R & D Canada |
| LCCM | Low-Cost Competent Munitions |
| NATO | North Atlantic Treaty Organization |
| OTAN | Organisation du Traité de l'Atlantique Nord |
| PE | Probable Error |
| SPACIDO | Système à Précision Améliorée par CInémomètre DOppler |
| STAR | Smart Trajectory Artillery Round |
| TCF | Trajectory Correction Fuze |

This page intentionally left blank.

## DOCUMENT CONTROL DATA

(Security classification of title, body of abstract and indexing annotation must be entered when the overall document is classified)

1. ORIGINATOR (The name and address of the organization preparing the document. Organizations for whom the document was prepared, e.g. Centre sponsoring a contractor's report, or tasking agency, are entered in section 8.)

Defence R&D Canada – Valcartier
2459 Pie-XI Blvd North
Quebec (Quebec)
G3J 1X5 Canada

2. SECURITY CLASSIFICATION (Overall security classification of the document including special warning terms if applicable.)

UNCLASSIFIED

3. TITLE (The complete document title as indicated on the title page. Its classification should be indicated by the appropriate abbreviation (S, C or U) in parentheses after the title.)

Low cost guidance and control solution for in-service unguided 155 mm artillery shell (U)

4. AUTHORS (last name, followed by initials – ranks, titles, etc. not to be used)

Gagnon, E.; Lauzon, M.

5. DATE OF PUBLICATION (Month and year of publication of document.)

July 2009

6a. NO. OF PAGES (Total containing information, including Annexes, Appendices, etc.)

54

6b. NO. OF REFS (Total cited in document.)

32

7. DESCRIPTIVE NOTES (The category of the document, e.g. technical report, technical note or memorandum. If appropriate, enter the type of report, e.g. interim, progress, summary, annual or final. Give the inclusive dates when a specific reporting period is covered.)

Technical Report

8. SPONSORING ACTIVITY (The name of the department project office or laboratory sponsoring the research and development – include address.)

Defence R&D Canada – Valcartier
2459 Pie-XI Blvd North
Quebec (Quebec)
G3J 1X5 Canada

9a. PROJECT OR GRANT NO. (If appropriate, the applicable research and development project or grant number under which the document was written. Please specify whether project or grant.)

Artillery precision guided munition / 12qj

9b. CONTRACT NO. (If appropriate, the applicable number under which the document was written.)

10a. ORIGINATOR'S DOCUMENT NUMBER (The official document number by which the document is identified by the originating activity. This number must be unique to this document.)

DRDC Valcartier TR 2008-333

10b. OTHER DOCUMENT NO(s). (Any other numbers which may be assigned this document either by the originator or by the sponsor.)

11. DOCUMENT AVAILABILITY (Any limitations on further dissemination of the document, other than those imposed by security classification.)

Unlimited

12. DOCUMENT ANNOUNCEMENT (Any limitation to the bibliographic announcement of this document. This will normally correspond to the Document Availability (11). However, where further distribution (beyond the audience specified in (11) is possible, a wider announcement audience may be selected.))

Unlimited

13. ABSTRACT (A brief and factual summary of the document. It may also appear elsewhere in the body of the document itself. It is highly desirable that the abstract of classified documents be unclassified. Each paragraph of the abstract shall begin with an indication of the security classification of the information in the paragraph (unless the document itself is unclassified) represented as (S), (C), (R), or (U). It is not necessary to include here abstracts in both official languages unless the text is bilingual.)

Guidance and control of artillery projectiles will be critical to future military operations. With the large quantities of unguided artillery shells stockpiled around the world, the course correction fuze could provide an attractive and cost-effective solution for munition control. This report proposes a drag brake and a spin brake course correction fuze concept, and compares their performance against the roll-decoupled four canard configuration. Specific guidance and control functions were designed and tuned for each using the 155 mm spin-stabilized artillery projectile as baseline. Dispersion sources included variations in muzzle velocity and gun's azimuth and elevation angles relative to nominal conditions, and wind velocity perturbations. Monte Carlo simulations were performed to analyze the delivery accuracy. Results show that the drag brake concept compensates for muzzle velocity and longitudinal wind perturbations efficiently. The spin brake concept compensates for perturbations in lateral wind efficiently and, to a lesser extent, in the gun's azimuth. The roll-decoupled four canard configuration counteracts gun's azimuth and elevation perturbations very well. A course correction fuze combining the drag brake and spin brake concepts is shown to be a good solution to increase the projectile accuracy when all disturbances studied are present.

14. KEYWORDS, DESCRIPTORS or IDENTIFIERS (Technically meaningful terms or short phrases that characterize a document and could be helpful in cataloguing the document. They should be selected so that no security classification is required. Identifiers, such as equipment model designation, trade name, military project code name, geographic location may also be included. If possible keywords should be selected from a published thesaurus, e.g. Thesaurus of Engineering and Scientific Terms (TEST) and that thesaurus identified. If it is not possible to select indexing terms which are Unclassified, the classification of each should be indicated as with the title.)

Guidance, Control, Weapon, Munition, Projectile, Shell, Missile, Artillery, Gunnery, Course correction fuze

**Defence R&D Canada**

Canada's Leader in Defence
and National Security
Science and Technology

**R & D pour la défense Canada**

Chef de file au Canada en matière
de science et de technologie pour
la défense et la sécurité nationale

DEFENCE R&D DÉFENSE

**www.drdc-rddc.gc.ca**